机器人多层多道焊缝激光视觉焊道的识别

张华军[1,2]， 张广军[1]， 蔡春波[2]， 高洪明[1]， 吴 林[1]
（1. 哈尔滨工业大学 现代焊接生产技术国家重点实验室，哈尔滨 150001；
2. 哈尔滨理工大学 材料科学与工程学院，哈尔滨 150040）

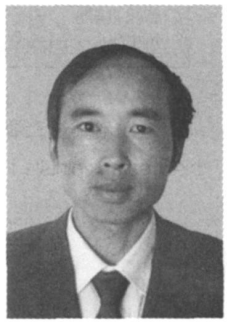

张华军

摘 要：厚板多层多道焊缝形状特征的自动识别，对保证焊接质量和实现机器人自动化焊接生产具有重要意义. 文中建立了基于条形激光源 CCD 视觉传感多道焊缝自动检测系统，通过对多道焊缝激光条纹图像特征的分析，提出了合理的图形处理识别流程，即经过图像平滑处理、纵向灰度梯度法识别条纹中心、再经过二重斜率平滑处理、多个峰值搜索等处理流程，可获得焊缝形状的四个拐点，为焊缝跟踪、弧长控制和焊枪位姿调整提供了重要的信息，其图像处理结果与试验结果相吻合.

关键词：多层多道焊；激光视觉；二重斜率平滑处理；图像处理；弧焊机器人
中图分类号：TP242 文献标识码：A 文章编号：0253－360X(2009)04－0105－04

0 序 言

大型厚板在船舶、高压容器等领域广泛应用，厚板结构一般采用多层多道焊，目前厚板结构焊接自动化程度低下，机器人焊接可以提高生产效率和焊接质量，是未来发展趋势[1]. 目前，针对厚板机器人焊接多采用完全示教的方法，其对工装精度和坡口加工精度要求非常高，该方法需要知道焊接参数与每道焊缝成形的定量关系，才能很好规划出每层每道的焊缝轨迹，由于厚板焊接结构产生较大的焊接变形[2,3]，严重影响厚板机器人焊接质量和自动化的实现. 因此，急需多层多道焊缝形状的检测系统来配合机器人完成焊接任务，由于直接进行 CCD 传感其识别难度大，并且易受弧光干扰[4]，目前采用激光作为主动光源 CCD 视觉传感可提取焊缝深度信息，抗干扰能力强而被采用[5]. 文中建立了基于条形激光源 CCD 视觉传感多道焊缝自动检测系统，重点研究多道焊缝激光条纹图像的处理和识别，得出合理的图像识别流程局部微调示教轨迹位置和姿态，最终满足焊接生产的需要.

1 系统的组成

整体系统主要由 Motoman 机器人系统、工控机、焊接设备、CCD 视觉传感器、滤光系统、条形激光源、图像采集卡及电源等组成. 其系统工作原理早有报道[5]，即采用面阵 CCD 视觉传感器拍摄激光焊缝条纹图像，通过 CG300 图像采集卡将图像传给工业控制机，经过数字图像处理识别焊缝，然后提取出多层多道焊缝形状特征参数，为多层多道焊接质量过程控制提供依据. 焊接试验采用熔化极气体保护焊，焊接顺序如图 1 所示，共有 4 层 9 道焊缝，每道焊接参数相同，板材为 Q235，焊丝为 E5015，焊丝直径 2.5 mm，板厚为 12 mm.

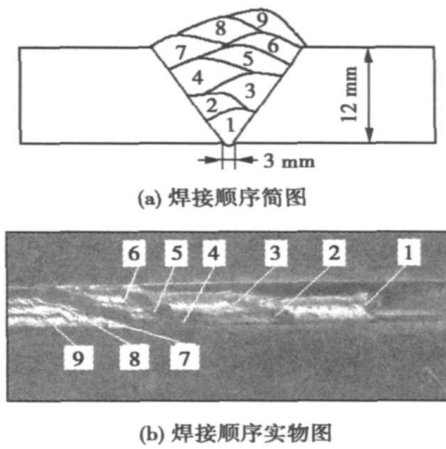

图 1 多层多道焊焊接顺序

Fig. 1 Multi-pass welding sequence

2 多层多道焊缝图像处理

2.1 图像采集及分析

视觉传感器采集的多道焊激光条纹图像如图 2

收稿日期：2008－01－14

所示，分别是第 3 ~ 6 道焊缝图像，可看出在前三层的焊缝两边缘拐点没有被填充，最后一层即第 6 道焊缝边缘右拐点被填充而消失，但会新产生一个右边缘拐点，焊缝底边始终有两个拐点，通过识别出焊缝上边缘两个拐点和焊缝底部两个拐点，就可将每道焊缝总体形状参数计算出来.

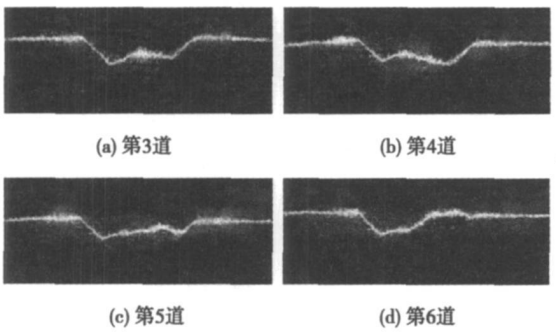

图 2 多层多道焊激光条纹图

Fig. 2 Laser strip of multi-pass welding seam

2.2 激光条纹图像处理流程

根据上述分析要求，针对多道焊激光条纹特征，设计的图像处理的流程如图 3 所示，采用纵向灰度梯度法快速的识别出焊缝激光条纹在横向上高度的分布矩阵，再采用多重斜率平滑处理获得了斜率变化曲线，通过对斜率曲线波峰和波谷的特征点进行搜索，可获得上述需要的四个特征点.

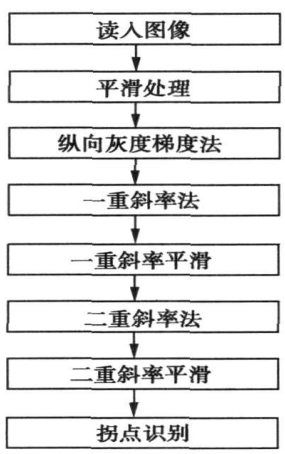

图 3 多道焊激光条纹图像处理流程

Fig. 3 Procedure of multi-pass laser image processing

2.3 图像识别算法推导

由于在实际焊接过程中存在有弧光和飞溅，对实时图像的采集影响很大，导致图像出现很多的噪声点，因而在提取特征点之前，应该对图像整体滤波去噪，图像增强. 采用平滑处理，就是要减少像素之间较大的差别，其原理公式如下，即

$$g(i,j)=\frac{1}{(2N+1)^2}\sum_{i=n}^{n+K}\sum_{j=m}^{m+K}f(i,j) \tag{1}$$

式中：K 为平滑系数；i，j 分别为图像的行和列变量；$f(i,j)$ 为原灰度函数；$g(i,j)$ 为柔化后的新灰度函数；n，m 分别为图像的行和列位置.

以第5道焊缝为例，从第100列纵向上灰度分布曲线如图 4a 可知，在焊缝中心处灰度最高，波峰对应的与 y 向位置即为激光条纹在纵向上的中心，其纵向处理后焊缝中心图像如图 4b 所示，其在 x 向上纵向位置分布矩阵存储在 $R(i)$ 中. 为了获得拐点，需要寻找出斜率突变点，采用多重斜率平滑处理算法可以获得其斜率变化曲线，其推导算法如下.

(1) 一重斜率法：

$$S_1(i)=\frac{1}{2N}\sum_{j=1}^{N}\frac{R(i+j)-R(i-j)}{2j} \tag{2}$$

(2) 一重平滑处理：

$$P_1(i)=\frac{1}{2M+1}\sum_{k=i-M}^{i+M}S_1(k)$$

$$=\frac{1}{2N(2M+1)}\sum_{k=i-M}^{i+M}\sum_{j=1}^{N}\frac{R(k+j)-R(k-j)}{2j} \tag{3}$$

(3) 二重斜率法：

$$S_2(i)=\frac{1}{2N}\sum_{j=1}^{N}\frac{P_1(i+j)-P_1(i-j)}{2j} \tag{4}$$

(4) 二重平滑处理：

$$P_2(i)=\frac{1}{2M+1}\sum_{k=i-M}^{i+M}S_2(k)$$

$$=\frac{1}{2M+1}\sum_{k=i-M}^{i+M}\frac{1}{2N}\sum_{j=1}^{N}\frac{P_1(k+j)-P_1(k-j)}{2j} \tag{5}$$

式中：N 为斜率平均因子；M 为平滑系数；k 为图像的位置变量；$R(i)$ 为图像第 i 列的灰度矩阵；$S_1(i)$ 为图像第 i 列的灰度一重斜率矩阵；$S_2(i)$ 为图像第 i 列的灰度二重斜率矩阵；$P_1(i)$ 为图像第 i 列的灰度一重斜率平滑处理后矩阵；$P_2(i)$ 为图像第 i 列的灰度二重斜率平滑处理后矩阵.

经过一重斜率法($N=4$)处理后，斜率曲线如图 4c 所示，存在大量的噪声，再经过一重平滑滤波($M=5$)如图 4d所示，噪声明显减少，但其峰值点不明显，再经过二重斜率平滑($N=8$；$M=5$)处理后，斜率曲线如图 4e 所示，四个峰值点 P_1 ~ P_4 都非常明显. 如果再经过三重斜率平滑($N=8$；$M=5$)处理后，斜率曲线如图 4f 所示，其峰值点又不明显了，因此，采用二重斜率平滑处理为最佳方案.

特征点的识别：如图 4e 所示，首先从左上角按照搜索方向 D_1 可识别出 P_1 点，再从 P_1 点正下方按照搜索方向 D_2 可识别出 P_2 点，以此类推，从右

下角按照搜索方向 D_3 可识别出 P_4 点, 再从 P_4 点正上方按照搜索方向 D_4 可识别出 P_3 点.

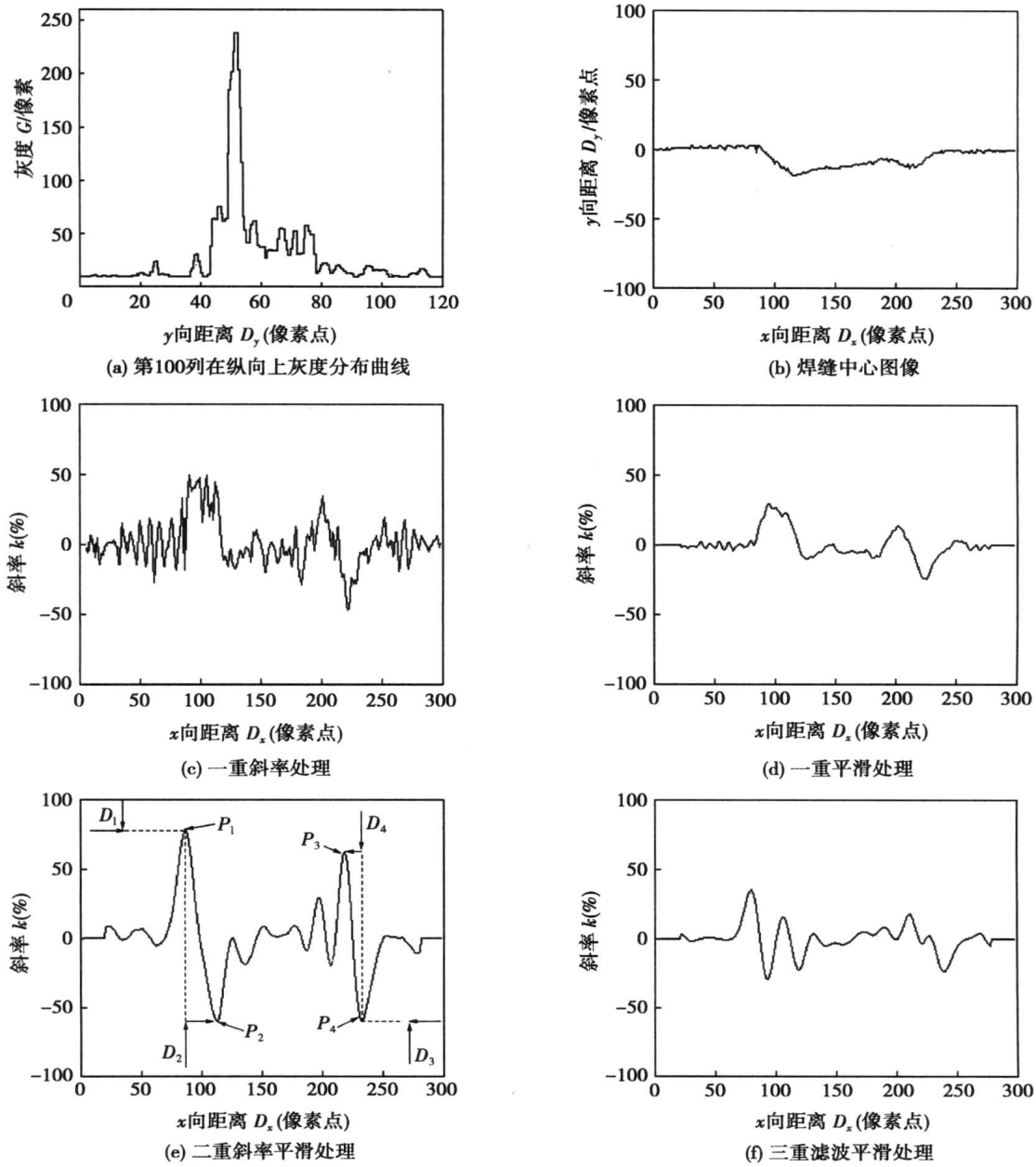

图 4　图像处理后曲线

Fig. 4　Diagram of image processing

3　试验结果

采用如图 3 图像处理识别流程, 分别对第 4, 5 和 6 道焊缝激光条纹进行处理和识别, 其识别结果如图 5 所示, 可以看出经过处理识别后的斜率曲线峰值 $P_1 \sim P_4$ 所对应的横坐标与焊缝边缘四个拐点位置基本相吻合. 根据这四个特征点可很好的确定待焊焊缝与焊枪高度, 还可确定出待焊焊缝中心与焊枪在焊缝宽度方向的偏移量, 以及确定出焊枪的工作角, 这些量对提高焊接质量具有很重要的意义. 也可对前焊道的填充效果进行检测, 可进行微调后续焊道的工艺参数, 使其获得预计的填充效果. 从第 6 道焊缝激光条纹来看, 其中坡口一个边缘已被焊缝填充上, 但还是会形成新的坡口, 还是有四个拐点, 通过识别这四个拐点, 可以提取焊缝坡口信息, 从而计算出焊枪与理论施焊位置的偏差量. 可看出该算法适应性强, 识别准确.

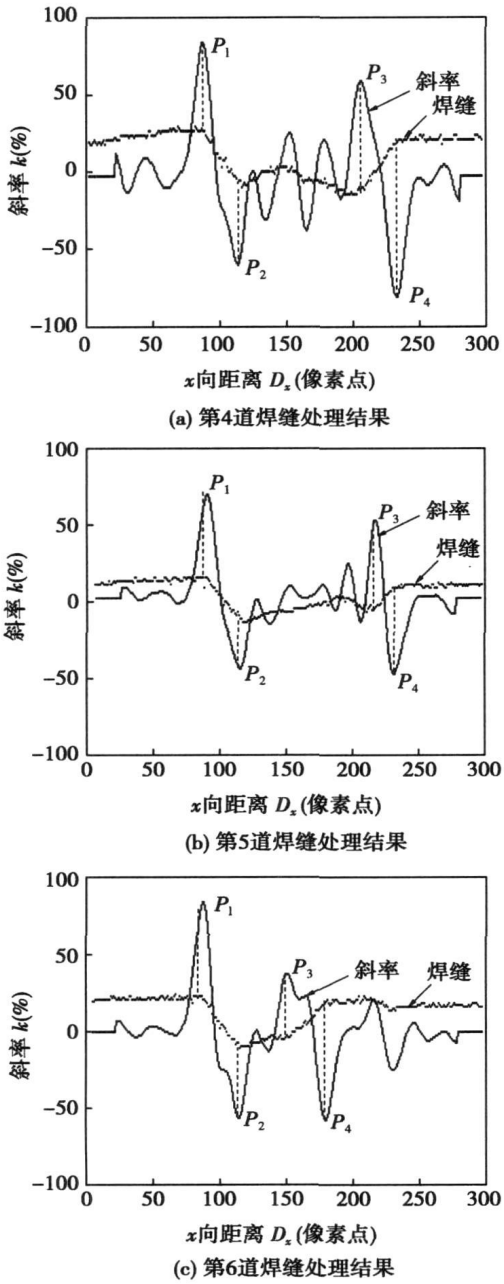

图 5 处理结果与试验结果对比

Fig. 5 Comparison of processed and experimental results

4 结 论

(1) 建立了基于激光视觉传感多层多道焊缝形状参数自动提取系统, 设计了最佳图像处理和识别流程, 其处理结果与试验结果相吻合.

(2) 采用并设计多重斜率平滑处理算法, 实现了对多层多道激光条纹四个拐点特征的自动提取, 为焊缝跟踪、弧长控制、焊枪位姿和后续焊接参数调整提供了重要的信息.

参考文献:

[1] 吴 林, 陈善本. 智能化焊接技术[M]. 北京: 国防工业出版社, 2000.

[2] 刘南生, 俞 进, 徐志锋, 等. 基于多层多道焊的弧焊机器人视觉信息提取及处理[J]. 南昌大学学报, 2005, 29(1): 63—66.
Liu Nansheng, Yu Jin, Xu Zhifeng, *et al*. The image processing of three-dimensional visual sensor based on multi-pass seam[J]. Journal of Nanchang University, 2005, 29(1): 63—66.

[3] Beattie R J, Cheng S K, Logue P S. The use of vision sensors in multipass welding applications[J]. Welding Journal, 1988(9): 28—33.

[4] 黄军芬, 殷树言, 邹 勇, 等. 多层焊填充层焊道图像处理及边缘提取[J]. 机械工程学报, 2005, 41(6): 133—136.
Huang Junfen, Yin Shuyan, Zou Yong, *et al*. Image processing and edge detection on multi-pass image[J]. Chinese Journal of Mechanical Engineering, 2005, 41(6): 133—136.

[5] 岳 宏, 孙立新, 蔡鹤皋. 基于结构光的机器人焊接实时图像处理方法的研究[J]. 机器人, 1999, 21(2): 144—147.
Yue Hong, Sun Lixin, Cai Hegao. Research on real time processing of robot welding image based on structure light[J]. Robot, 1999, 21(2): 144—147.

作者简介: 张华军, 男, 1978 年出生, 博士研究生, 讲师. 主要从事高效焊接工艺及机器人智能化焊接技术的研究. 发表论文 20 篇.

Email: huajunzhang@126.com

(State Key Laboratory of Advanced Welding Production Technology, Harbin Institute of Technology, Harbin 150001, China). p93—96

Abstract: Tensile strength, bending strength, impact toughness and non-destructive inspection tests of TIG welded 20G/316L clad pipe joint were carried out. The microstructure and the diffusion of the major alloying elements were analysed using optical microscopy, SEM and chemical analysis. The results showed that the weld can be divided into four layers including carbon steel layer, diffusion layer, transition layer and stainless steel layer. The microstructure in diffusion layer was characterized by the martensite and retained austenite. The transition layer only contained austenite, and the stainless steel layer included afterbirth-like crystal. The defect-free joint was produced and performed well under the experimental parameters. The concentration of nickel and chromium element in weld root did not decrease compared with the corresponding welding materials, which proved that the employment of transition welding wire could maintain the concentration of the major alloying elements in welding root.

Key words: 20G/316L clad pipe; TIG; microstructure; mechanical properties

Quality evaluation of the resistance spot welding based on PCA-SVM ZHANG Hongjie[1], HOU Yanyan[2] (1. School of Machinery and Electron, Tianjin Polytechnic University, Tianjin 300160, China; 2. Department of Architecture Engineering, Hebei College of Administration, Shijiazhuang 050031, China). p97—100

Abstract: The electrode displacement and dynamic resistance signals of resistance spot welding process are collected synchronously. Through the time-domain analysis of electrode displacement signal in the welding process, nine characteristic parameters relating to weld quality are picked up to set up a set of data which characterizes the input samples, on the basis of the different phase of nugget forming marked by simultaneous dynamic resistance signal. The principal component analysis (PCA) to remove the self-correlation of input characteristics and realize dimensionality reduction is integrated with the conventional method of support vector machine(SVM), while the shear strength of welded spot was taken as the evaluation index of welded spot quality. The comparison of predicted results under PCA-SVM and conventional SVM by means of cross-validation test shows that PCA-SVM algorithm improves the generalization ability and the predicted accuracy of SVM method.

Key words: resistance spot welding; principal component analysis; support vector machine; regression analysis

Numerical simulation of the temperature field during resistance spot welding with rectangular electrode ZHANG Xiaoqi[1,2], XU Guocheng[1], WANG Chunsheng[1,3], WEN Jing[1] (1. School of Material Science and Engineering, Jilin University, Changchun 130025, China; 2. Jilin Teachers Institute of Rnqineeriy and Fechnology, Changchen 130052, China; 3. Changchun Railway Vehicles Corporation, Changchun 130062, China). p101—104

Abstract: The temperature field during resistance spot welding with rectangular electrode was simulated using ANSYS. The physical model was properly simplified on the basis of simulation accuracy and technological conditions. One-quarter three-dimensional finite element model during resistance spot welding was built in which the contact resistance was substituted by the electric resistivity. The results show that at the beginning of welding, the edge of electrodes has the highest temperature because of high stress induced by the electrode force. As welding time is longer, the contact resistance decreases and the highest temperature position moves to inside, the nugget appears to be similar with the conventional spot welding.

Key words: rectangular electrode; numerical simulation; temperature field

Laser-based visual recognition of multi-pass seam in robot arc welding ZHANG Huajun[1,2], ZHANG Guangjun[1], CAI Chunbo[2], GAO Hongming[1], WU Lin[1] (1. State Key Laboratory of Advanced Welding Production Technology, Harbin Institute of Technology, Harbin 150001, China; 2. College of Material Science and Engineering, Harbin University of Science and Technology, Harbin 150040, China). p105—108

Abstract: It is very necessary for the improvement of weld quality and the realization of robot automatic production to detect multi-pass weld profile parameters automatically. Automatic detective system of multi-pass weld profile parameters by band laser visual sensor was developed. The procedure of image process is as follows: smoothing, center recognition by longitudinal grey gradient, twice slope smooth process, and multiple peaks search by laser seam image analysis. It is very important for seam tracking, arc length control and torch attitude adjustment to obtain four character points of weld seam profile. And the recognition results agree with the experimental results.

Key words: multipass welding; laser visual sensor; image process; twice slope smooth process; robot arc welding

Research on gravity compensation algorithm for tool-assembling with force control in remote welding WEI Xiuquan, WU Lin, GAO Hongming, LI Haichao (State Key Laboratory of Advanced Welding Production Technology, Harbin Institute of Technology, Harbin 150001, China). p109—112

Abstract: Based on the control strategy of global teleoperative and local autonomous, a tool-assembling experimental system with force control for remote welding is established. The tool gravity calculation and linear least-squares algorithm are adopted to calibrate the tool load parameter, and a tool gravity compensation algorithm based on the tool load parameter vector is proposed to eliminate the gravity disturbance during the tool-assembling process with force control. For a customized assembing tool, experiments on load parameter calibration and gravity compensation in non-contact condition are carried out. The experimental results show that the tool gravity compensation algorithm can obtain a high precision, meeting the requirements of local autonomous force control in tool-assembing task, while the maximum error of gravity compensation and gravity moment compensation are 1 N and 0.1 N·m, respectively.

Key words: gravity compensation; force control; tool assembling; remote welding